Fluorogenic Probes

DOI: 10.1002/anie.201403890

Ultrafluorogenic Coumarin–Tetrazine Probes for Real-Time Biological Imaging**

*Labros G. Meimetis, Jonathan C. T. Carlson, Randy J. Giedt, Rainer H. Kohler, and Ralph Weissleder**

Abstract: *We have developed a series of new ultrafluorogenic probes in the blue-green region of the visible-light spectrum that display fluorescence enhancement exceeding 11 000-fold. These fluorogenic dyes integrate a coumarin fluorochrome with the bioorthogonal trans-cyclooctene(TCO)–tetrazine chemistry platform. By exploiting highly efficient through-bond energy transfer (TBET), these probes exhibit the highest brightness enhancements reported for any bioorthogonal fluorogenic dyes. No-wash, fluorogenic imaging of diverse targets including cell-surface receptors in cancer cells, mitochondria, and the actin cytoskeleton is possible within seconds, with minimal background signal and no appreciable non-specific binding, opening the possibility for in vivo sensing.*

One of the major challenges in clinical medicine and biomedical research remains the accurate detection of abnormal cellular and subcellular events. This is particularly important in the detection of rare cancer cells in a sea of normal host cells,[1] for improved diagnostic performance in point-of-care devices,[2] in detecting invading tumor margins during surgery,[3] in determining drug effects at the single-cell level,[4] or for the detection of aberrant proteins. There have been tremendous advances in the development of optical sensing approaches but what is still generally lacking are efficient, cell-permeable, and biocompatible fluorochromes with zero background signal. With most diagnostic readouts (e.g. cytopathology, flow cytometry, microscopy) the background fluorescence of fluorochrome-tagged affinity ligands is always a concern, necessitating careful optimization of staining conditions and extensive washing steps. While this is feasible in larger sample sizes where washing steps are well tolerated, it becomes much more difficult with scant cell populations (for example circulating tumor cells, stem cells, immune cell subtypes), in microfluidic point-of-care devices where cell-washing steps are more difficult to incorporate, and in the labeling of small molecules, whose properties are frequently perturbed by fluorescent tags. For these reasons, new fluorochromes with zero background signal but extensive bioorthogonal amplification are needed.

Pioneering work has built probes around the Staudinger ligation and azide–alkyne cycloaddition "click" platforms that have principally employed photoinduced electron transfer (PET) or Förster resonance energy transfer (FRET) as a means to suppress fluorescence emission.[5] Unfortunately, in spite of laborious design efforts to customize quenching mechanisms for a given fluorophore system, the modest brightness enhancement of these probes (typically less than 30-fold) yields relatively poor target-to-background ratios and thus limits their utility in vivo. More recently, we reported on BODIPY–tetrazine conjugates that achieved higher amplifications (up to 1600-fold) in the green region of the light spectrum by through-bond energy transfer (TBET).[6] By providing a conduit for energy transfer within a contiguous scaffold of π bonds, TBET circumvents many of the solvent, spatial, and spectral limitations that PET and FRET exhibit and can yield very high efficiencies.[7] However, multicolor TBET probes have not been synthesized to date. Eager to extend the current armamentarium of cell-permeable and biocompatible ultrafluorogenic probes, we set out to systematically develop a series of bioorthogonal HELIOS probes in the blue-green region of the visible-light spectrum (HELIOS = hyperemissive ligation-initiated orthogonal sensing). Herein, we report a series of these molecules with the highest reported emission turn-on ratios.

Coumarin fluorochromes are small and biocompatible, and are widely used for in vivo and in vitro diagnostics and imaging.[8] They cover an extensive spectral range, with the brightest fluorochromes undergoing excitation and emission in the blue spectral region. Coumarin 102 (**1**; Scheme 1) was initially selected as it has a high quantum yield in water ($\Phi = 0.66$),[9] a peak absorbance compatible with $\lambda = 405$ nm laser excitation, and a previously described transition dipole[10] relevant to rational probe design. Energy transfer and fluorogenic switching should be maximized by collinear alignment of the emission transition dipole of coumarin 102 (**1**) with the absorption transition dipole of tetrazine, which is perpendicular to the heterocyclic plane (Figure 1 a).[11]

Although several synthetic approaches are possible we postulated that appending a phenyltetrazine at the C3 position of **1** would allow for efficient TBET, and that the *meta* configuration would yield maximum fluorescence attenuation. To this end, **1** was brominated using the reagent *N*-bromosuccinimide, followed by a Suzuki coupling with 3-cyanophenylboronic acid in the presence of the catalyst $[Pd(OAc)_2(PPh_3)_2]$, heating the reaction to reflux in a mixture

[*] Dr. L. G. Meimetis,[+] Dr. J. C. T. Carlson,[+] Dr. R. J. Giedt, Dr. R. H. Kohler, Prof. R. Weissleder
Center for Systems Biology
Massachusetts General Hospital
185 Cambridge Street, Boston, MA 02114 (USA)
E-mail: rweissleder@mgh.harvard.edu

[+] These authors contributed equally to this work.

[**] Part of this work was supported by National Institutes of Health grant number R01EB01011. We thank Dr. Katy Yang for cell-culture assistance and Alex Zaltsman for microscopy assistance.

Supporting Information for this article is available on the WWW under http://dx.doi.org/10.1002/anie.201403890.

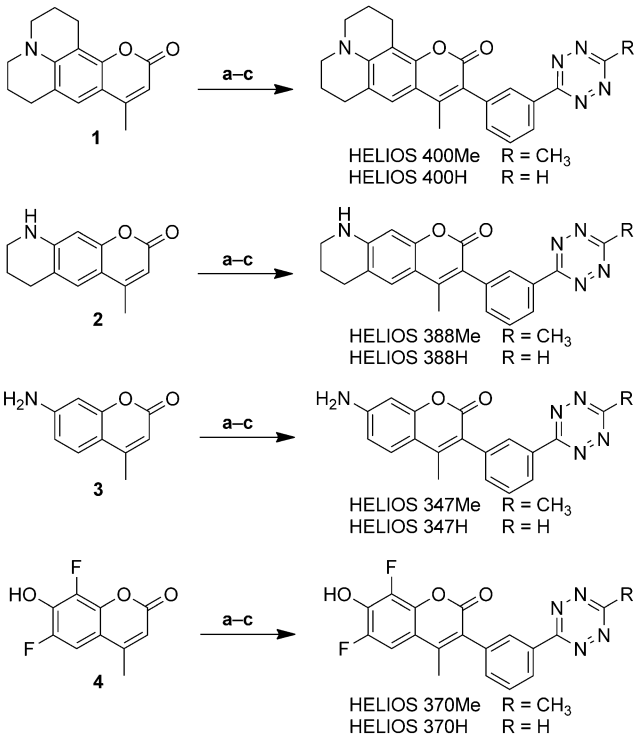

Scheme 1. Synthesis of bioorthogonal fluorogenic HELIOS probes. Reagents and conditions: a) *N*-Bromosuccinimide in acetonitrile; b) 3-cyanophenylboronic acid, $[Pd(OAc)_2(PPh_3)_2]$, K_2CO_3 in 75% dioxane (in water) at 100°C; c) hydrazine, $Zn(OTf)_2$, acetonitrile/dioxane (Me-Tz) or formamidine hydrochloride/DMF (H-Tz) at 60°C for 15 h followed by $NaNO_2$ and HCl.

of dioxane/water (see Supporting Information). The resultant nitrile was taken up in dioxane and was treated with hydrazine, $Zn(OTf)_2$, and acetonitrile, and subsequently heated to 60°C.[12] Treatment of the crude mixture with sodium nitrite, followed by an acidic workup furnished the corresponding methyltetrazine HELIOS 400Me in three steps from commercially available starting materials (Scheme 1). As a mechanistic control, we constructed the *para*-substituted tetrazine analogue HELIOS 400*p*Me by a parallel route (see the Supporting Information). The transition dipoles between donor and acceptor of this probe are nearly perpendicular and would thus be predicted to yield negligible quenching by FRET (Figure 1a). Measuring the emission turn-on of HELIOS 400*p*Me relative to *meta*-substituted HELIOS 400Me provides a facile method to validate TBET as the underlying mechanism for fluorescence quenching.

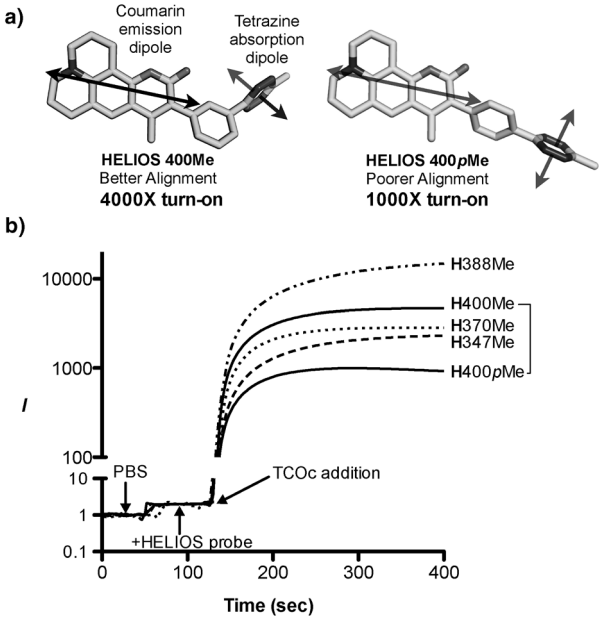

Figure 1. a) The approximate transition dipole orientation between coumarin 102 (**1**)[10] and tetrazine[11] in HELIOS 400Me and HELIOS 400*p*Me. b) Fluorogenic activation timecourse of HELIOS probes upon reaction with TCOc (**H** = HELIOS).

HELIOS 400Me and HELIOS 400*p*Me were both soluble in phosphate-buffered saline (PBS) at micromolar concentrations and were negligibly fluorescent in their native state. After rigorous purification to remove trace fluorescent impurities, we evaluated the fluorogenic properties of these new coumarin–Tz conjugates (Tz = tetrazine) on reaction with TCOc (a *trans*-cyclooctene derivative), which incorporates a carbamate-linked PEG_2 side chain for improved water solubility (see Supporting Information). Addition of TCOc to HELIOS 400Me in PBS yielded a fluorescence peak turn-on ratio of 4000-fold (Figure 1b). Reaction of HELIOS 400*p*Me with TCOc yielded a turn-on ratio of 1000-fold, four-times lower than its *meta*-linked counterpart. Mechanistically, the detection of 1000-fold emission turn-on in a perpendicular-dipole configuration argues against FRET playing a significant role in the energy transfer mechanism.[13] Furthermore, the fluorescence emission intensity of the native probes was found to be independent of solvent polarity, which suggests that PET is not the operative photophysical quenching mechanism for these probes (Figure S1, Supporting Information).

Encouraged by this outcome, we next implemented this design in a series of structurally diverse coumarins that span the full blue spectral range (Figure 2a). Dyes known to retain bright fluorescence emission in aqueous solution were again selected, including coumarin 339 (**2**),[14] coumarin 120 (**3**), and difluorinated hydroxycoumarin **4**[15](Scheme 1). The same modular synthetic approach involving bromination, Suzuki coupling, followed by metal-catalyzed tetrazine formation was used to generate this small library of coumarin–Tz conjugates (Scheme 1). HELIOS 388Me in PBS yielded a remarkable 11000-fold fluorescence turn-on upon reaction with TCOc, the highest turn-on ratio reported to date. When ligated to TCOc in PBS, HELIOS 347Me and HELIOS 370Me displayed 2500-fold and 2900-fold turn-on ratios, respectively, in spite of minimal spectral overlap with the tetrazine absorption band at $\lambda = 520$ nm. By comparison, FRET-based coumarin–tetrazine interactions are dramatically less efficient: a flexibly linked analogue of HELIOS 370H displayed only a 60-fold turn-on (Marina Blue-Tz, see the Supporting Information), corroborating the dipole-orientation analysis above. All four HELIOS probes exhibit very good post-click quantum yields in PBS (upon

ligation with TCOc), in agreement with structurally similar coumarins (Table 1).

To demonstrate the applicability of these probes as native bioorthogonal fluorogenic imaging agents, we used HELIOS 370H. We chose a simple model system to assess HELIOS probe kinetics in the extracellular context: imaging of the epidermal growth factor receptor (EGFR) on the surface of cancer cells. EGFR overexpression plays a critical role in the most common molecularly defined subtype of lung cancer, where it is a key treatment target, and drives proliferation in other epithelial malignancies, including colon cancer and pancreatic cancer.[16] A431 cells were incubated with a TCO labeled anti-EGFR antibody (20 μg mL^{-1}, Cetuximab, ImClone) for 20 min and then washed briefly with PBS. Addition of 100 nM HELIOS 370H in PBS revealed bright, membrane-specific staining coinciding with the known distribution of the receptor (Figure 2c). Images were generated within seconds of dye addition and exhibited no nonspecific binding even after extended incubation, and no membrane staining in the presence of a control antibody–TCO conjugate (see the Supporting Information).

To further explore the imaging potential of HELIOS probes, we selected mitochondria as a target; their structures have features at the diffraction limit of conventional light microscopy. OVCA-429 cells expressing mitochondria-specific red fluorescent protein (RFP) were incubated with an anti-mitochondria antibody–TCO conjugate and were visualized with HELIOS 388H, yielding high-spatial-resolution images with good colocalization (Figure 3a). Intracellular imaging of small molecule targets is another area of intense interest, given the potential applications in drug

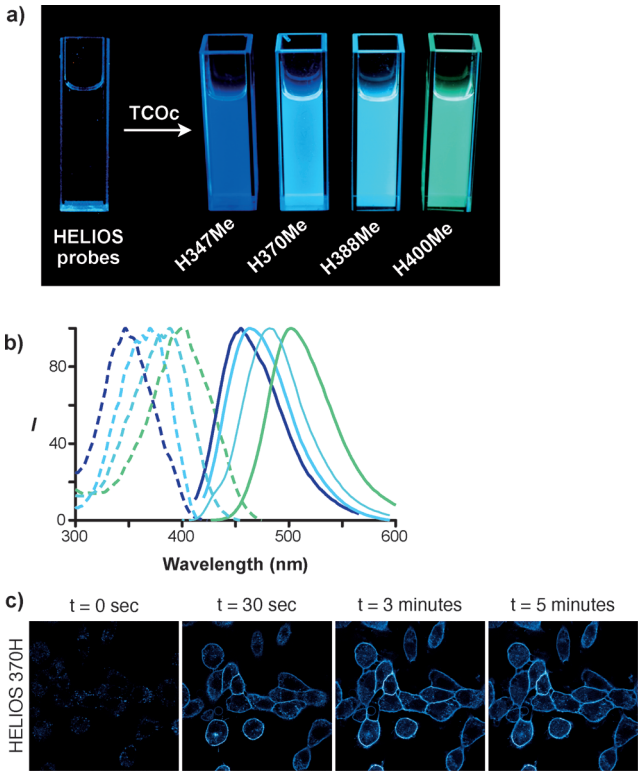

Figure 2. a) Visualization of the turn-on response using a handheld UV lamp. Left: cuvette containing HELIOS 347Me in PBS. Right: cuvettes with individual HELIOS probes (from left to right: H347Me, H370Me, H388Me, and H400Me) and TCOc in PBS. b) Normalized absorption and emission spectra of clicked products in PBS. c) No-wash fluorogenic imaging of EGFR expression on A431 cells. Cells were incubated with an α-EGFR–TCO antibody (20 mcg mL^{-1}), washed briefly, and then imaged sequentially after addition of 100 nM HELIOS 370H in PBS. Bright, membrane-specific staining is visible within seconds, reaches a maximum within 3 min and is stable thereafter.

Table 1: Photophysical Properties.

Probe	$\lambda_{ex}/\lambda_{em}$ [nm]	ε [cm^{-1}M^{-1}][a]	Φ[b]	Fluorescence Enhancement[c]
HELIOS 400	400/502	16000	0.41	4000-fold
HELIOS 388	388/482	20000	0.38	11000-fold
HELIOS 370	370/463	19000	0.49	2900-fold
HELIOS 347	347/455	18500	0.29	2500-fold
Marina Blue-Tz	362/459	ND	ND	60-fold

[a] At peak excitation wavelength in PBS, pH 7.4. [b] Quantum yield for the dihydropyridazine product after complete reaction of the indicated compound with TCOc in PBS at pH 7.4; quinine sulfate in H_2SO_4 (0.5 M, $\Phi = 0.546$) was used as the standard. [c] Fluorogenic turn-on ratio of the Me-tetrazines upon reaction with TCOc. ND = not determined.

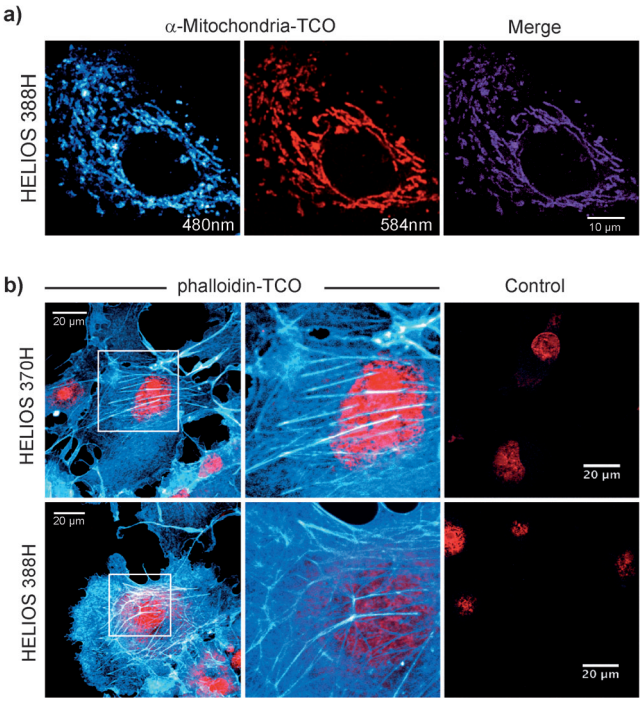

Figure 3. No-wash fluorogenic imaging of intracellular targets. a) Mitochondrial imaging: OVCA-429 cells with RFP-tagged mitochondria were incubated with an anti-mitochondria-TCO antibody, rinsed briefly, and then imaged after addition of 100 nM HELIOS 388H in PBS. Colocalization analysis in ImageJ (Costes auto-threshold) was used to generate the merged image in the right-hand panel (scale bar = 10 μm). b) Actin imaging: COS-1 cells were incubated with phalloidin–TCO (1 μg mL^{-1}) and DRAQ5 nuclear counterstain (1 μM, BioStatus), rinsed briefly, and then imaged upon addition of the indicated HELIOS probe at 100 nM. Control images were collected at matched dye concentrations in the absence of phalloidin–TCO (scale bars = 20 μm).

development, chemical biology, and optical pharmacology. To demonstrate the utility of HELIOS probes in this context with a structurally validated model system, we tested their ability to image the actin cytoskeleton with a phalloidin–TCO conjugate (see the Supporting Information). Sequential addition of phalloidin–TCO and several HELIOS probes produced vivid fluorogenic images of the cytoskeleton; control experiments revealed negligible background (Figure 3b).

In summary, the library of turn-on HELIOS probes spans the visible-light spectrum from blue to green, providing appealing optical flexibility for imaging applications and validating the generality and robustness of the TBET-tetrazine mechanism. The fast, catalyst-free, and exceptionally fluorogenic reactivity of these probes should synergize with emerging methods for facile dienophile labelling of biological targets, including metabolically incorporated cyclopropenes[17] and TCO-amino acids.[18] We believe this series of HELIOS dyes will prove useful in vitro, in vivo, and in diagnostic settings, in addition to enhancing methods for super-resolution microscopy.

Received: April 1, 2014
Published online: June 10, 2014

Keywords: click chemistry · coumarin dyes · energy transfer · fluorescence probes · tetrazines

[1] A. V. Ullal, V. Peterson, S. S. Agasti, S. Tuang, D. Juric, C. M. Castro, R. Weissleder, *Sci. Transl. Med.* **2014**, *6*, 219ra9.
[2] V. M. Peterson, C. M. Castro, J. Chung, N. C. Miller, A. V. Ullal, M. D. Castano, R. T. Penson, H. Lee, M. J. Birrer, R. Weissleder, *Proc. Natl. Acad. Sci. USA* **2013**, *110*, E4978.
[3] G. M. van Dam et al., *Nat. Med.* **2011**, *17*, 1315.
[4] G. M. Thurber, K. S. Yang, T. Reiner, R. H. Kohler, P. Sorger, T. Mitchison, R. Weissleder, *Nat. Commun.* **2013**, *4*, 1504.
[5] K. Sivakumar, F. Xie, B. M. Cash, S. Long, H. N. Barnhill, Q. Wang, *Org. Lett.* **2004**, *6*, 4603; N. K. Devaraj, S. Hilderbrand, R. Upadhyay, R. Mazitschek, R. Weissleder, *Angew. Chem. Int. Ed.* **2010**, *49*, 2869; *Angew. Chem.* **2010**, *122*, 2931; J. C. Jewett, C. R. Bertozzi, *Org. Lett.* **2011**, *13*, 5937; P. Shieh, M. J. Hangauer, C. R. Bertozzi, *J. Am. Chem. Soc.* **2012**, *134*, 17428.
[6] J. C. T. Carlson, L. G. Meimetis, S. A. Hilderbrand, R. Weissleder, *Angew. Chem. Int. Ed.* **2013**, *52*, 6917; *Angew. Chem.* **2013**, *125*, 7055.
[7] S. Speiser, *Chem. Rev.* **1996**, *96*, 1953.
[8] C. Uttamapinant, K. A. White, H. Baruah, S. Thompson, M. Fernández-Suárez, S. Puthenveetil, A. Y. Ting, *Proc. Natl. Acad. Sci. USA* **2010**, *107*, 10914; G. Signore, R. Nifosì, L. Albertazzi, B. Storti, R. Bizzarri, *J. Am. Chem. Soc.* **2010**, *132*, 1276.
[9] G. Jones, W. R. Jackson, C. Y. Choi, W. R. Bergmark, *J. Phys. Chem.* **1985**, *89*, 294.
[10] M. Theisen, M. Linke, M. Kerbs, H. Fidder, M. E.-A. Madjet, A. Zacarias, K. Heyne, *J. Chem. Phys.* **2009**, *131*, 124511.
[11] T. G. Kim, J. C. Castro, A. Loudet, J. G.-S. Jiao, R. M. Hochstrasser, K. Burgess, M. R. Topp, *J. Phys. Chem. A* **2006**, *110*, 20.
[12] J. J. Yang, M. R. Karver, W. W. Li, S. S. Sahu, N. K. Devaraj, *Angew. Chem. Int. Ed.* **2012**, *51*, 5222; *Angew. Chem.* **2012**, *124*, 5312.
[13] L. Giribabu, A. Ashok Kumar, V. Neeraja, B. G. Maiya, *Angew. Chem. Int. Ed.* **2001**, *40*, 3621; *Angew. Chem.* **2001**, *113*, 3733; J. R. Lakowicz, *Principles of Fluorescence Spectroscopy*, Springer, Heidelberg, **2009**, p. 954.
[14] R. L. Atkins, D. E. Bliss, *J. Org. Chem.* **1978**, *43*, 1975.
[15] C. Hedberg, F. J. Dekker, M. Rusch, S. Renner, S. Wetzel, N. Vartak, C. Gerding-Reimers, R. S. Bon, P. I. H. Bastiaens, H. Waldmann, *Angew. Chem. Int. Ed.* **2011**, *50*, 9832; *Angew. Chem.* **2011**, *123*, 10006.
[16] F. Ciardiello, G. Tortora, *N. Engl. J. Med.* **2008**, *358*, 1160.
[17] C. M. Cole, J. Yang, J. Šečkutė, N. K. Devaraj, *ChemBioChem* **2013**, *14*, 205; D. M. Patterson, L. A. Nazarova, B. Xie, D. N. Kamber, J. A. Prescher, *J. Am. Chem. Soc.* **2012**, *134*, 18638; J. Yang, J. Šečkutė, C. M. Cole, N. K. Devaraj, *Angew. Chem. Int. Ed.* **2012**, *51*, 7476; *Angew. Chem.* **2012**, *124*, 7594.
[18] I. Nikić, T. Plass, O. Schraidt, J. Szymański, J. A. G. Briggs, C. Schultz, E. A. Lemke, *Angew. Chem. Int. Ed.* **2014**, *53*, 2245; *Angew. Chem.* **2014**, *126*, 2278.

